

---

# LegoFormer: Transformers for Block-by-Block Multi-view 3D Reconstruction

---

Farid Yagubbayli<sup>1</sup>  
farid.yagubbayli@tum.de

Alessio Tonioni<sup>2</sup>  
alessiot@google.com

Federico Tombari<sup>1,2</sup>  
tombari@in.tum.de

<sup>1</sup>Technical University of Munich

<sup>2</sup>Google Inc.

## Abstract

Most modern deep learning-based multi-view 3D reconstruction techniques use RNNs or fusion modules to combine information from multiple images after encoding them. These two separate steps have loose connections and do not consider all available information while encoding each view. We propose LegoFormer, a transformer-based model that unifies object reconstruction under a single framework and parametrizes the reconstructed occupancy grid by its decomposition factors. This reformulation allows the prediction of an object as a set of independent structures then aggregated to obtain the final reconstruction. Experiments conducted on ShapeNet display the competitive performance of our network with respect to the state-of-the-art methods. We also demonstrate how the use of self-attention leads to increased interpretability of the model output.

## 1 Introduction

The fast-paced developments in the fields of robotic perception, 3D object modeling and augmented reality demand efficient, accurate, and interaction-less multi-view 3D reconstruction. Traditional approaches based on Structure-from-Motion (SfM) [20] and Simultaneous Localization and Mapping (SLAM) [10] focus on determining explicit solutions based on multi-view geometry by proposing different derivations of the underlying mathematical model of 3D-to-2D projections. One of their limitations is that they either fail or generate only partial shapes when only a few primarily non-overlapping views are available due to the violation of the camera pose / overlapping views and object surface assumptions. At the same time, this situation frequently occurs within the aforementioned application scenarios: e.g., in 3D object modeling for online shopping only a small number of images from uncalibrated cameras are available, taken under a high variability of lighting conditions. Although prior knowledge-based techniques [17, 33] can help to relax the assumptions, a large database of shape priors and handcrafted conditioning makes them less viable in practice.

Recently, several CNN-based techniques were proposed to reconstruct objects as a voxel grid from few uncalibrated images with limited coverage. Methods like 3D-R2N2 [5] and LSM [13] treat multiple views as a sequence and utilize modified RNN models to fuse information from different views. The use of RNNs comes with drawbacks, such as long processing times, the difficulty of processing longer input sequences, and the dependence of the output from the input sequence order. More recent works [30, 31] proposed solutions that replace the RNN model with a dedicated fusion module which improves performance by considering all views simultaneously and avoid "forgetting" earlier ones. However, only one view at a time is considered during the encoding phase because the view encoding, model prediction and fusion stages are separate. This also increases the complexity of training such networks since the modules need to be trained progressively [30]. Lastly, all prior work predicts every voxel in the output 3D volume individually which can lead to undesirable reconstructions unless structural properties like smoothness and continuity are not enforced explicitly.

To address these drawbacks, we propose LegoFormer - a model that uses a transformer network [26] to jointly encode all views and predict a 3D reconstruction in the form of its tensor decomposition. Figure 1 illustrates a high-level overview of the LegoFormer architecture. We argue that transformers are particularly suited to the task at hand since their attention mechanism allows exploiting information from all views while encoding a specific one, thus enriching its learned representation. This is in contrast with previous work based on CNNs and RNNs, where the knowledge from all views becomes available only once the encoding phase ends. Moreover, as most of the reconstructed objects are man-made, they are expected to have a certain regular structure which can be leveraged to use more efficient representations based on tensor decomposition. To this end we represent a voxel grid  $V \in \mathbb{R}^{N \times N \times N}$  by  $k$  decomposition factors of size  $\mathbf{d} \in \mathbb{R}^{3 \times N}$ . The decoder part of our architecture takes a set of learned encoded queries as input and transforms each one into a set of three vectors (the decomposition factors). Taking a cross-product between each triplet of vectors gives a rank-1 estimation of the output voxel grid. Different queries generate different estimations corresponding to different parts of the object, e.g., the legs of a table or the backrest of a chair; combining the parts together generates the final voxel volume. Therefore our network learns to predict objects as a sum of independent parts in a completely unsupervised way. For the special case of only one input view available, the attention across views cannot be computed. Therefore, we also propose an architecture tailored for this use case, where patches from the same image are used as encoder inputs similarly to what done in Vision Transformer (ViT) [7]. To differentiate between the two cases, the models are respectively named LegoFormer-M (multi-view) and LegoFormer-S (single-view).

To summarize our contributions:

- We introduce LegoFormer, a novel architecture for single- and multi-view object reconstruction that uses self-attention for both jointly encoding the input views and predicting the output volume.
- We propose to parametrize the output grid by its decomposition factors to take advantage of the inherent structures in common objects, and reformulate the task as the prediction of these factors.
- We show how LegoFormer learns to decompose a shape into a sum of tensor decomposition factors without explicit supervision for it.

We evaluate our proposal on ShapeNet showing competitive performance against prior techniques. Thanks to our tensor decomposition-based output and to the use of the attention mechanism, our models show desirable properties like a smoother and regular output, and a significant increase on the interpretability of the reconstructions.

## 2 Previous work

**3D Reconstruction** Classical techniques like SfM [20] and SLAM [10] rely on feature extraction and matching across different views. Both steps assume highly overlapping views and Lambertian surfaces that limit their use. With the availability of large 3D object datasets and advances in deep learning, a new category of learned methods emerged. The majority of techniques for multi-view 3D reconstruction [5, 13, 30, 31] use an encoder-decoder architecture to map 2D images into 3D volumes. The mapping is done individually on each image therefore discarding information shared among views. Methods like 3D-R2N2 [5] and LSM [13] introduce recurrent models to combine information from individual 3D volumes into a single volume, while Pix2Vox [30, 31] uses a dedicated fusion unit. [24] regresses the view poses and uses silhouettes to build an initial volume, then, as also done in LSM and Pix2Vox, uses a refiner unit that makes corrections to the predicted volumes based on the shape priors acquired during training. In contrast to these works, LegoFormer combines encoding, fusion, and decoding under a single transformer model. This structure allows the use of information from all the views in every stage of the process, resulting in a more tightly integrated framework.

**Transformers** Transformers have shown enormous success in a large variety of NLP tasks since their introduction by [26]. Recent work started to utilize transformer models for computer vision tasks by reformulating the inputs, which are mostly 2D RGB images, as a sequence of tokens [7, 4, 2]. ViT [7] is one of the earliest image classification methods that use a transformer encoder directly on a sequence of image patches. DETR [4] combines a pre-trained CNN backbone with an encoder-decoder transformer and predicts a sequence of bounding boxes in parallel. TimeSformer [2]

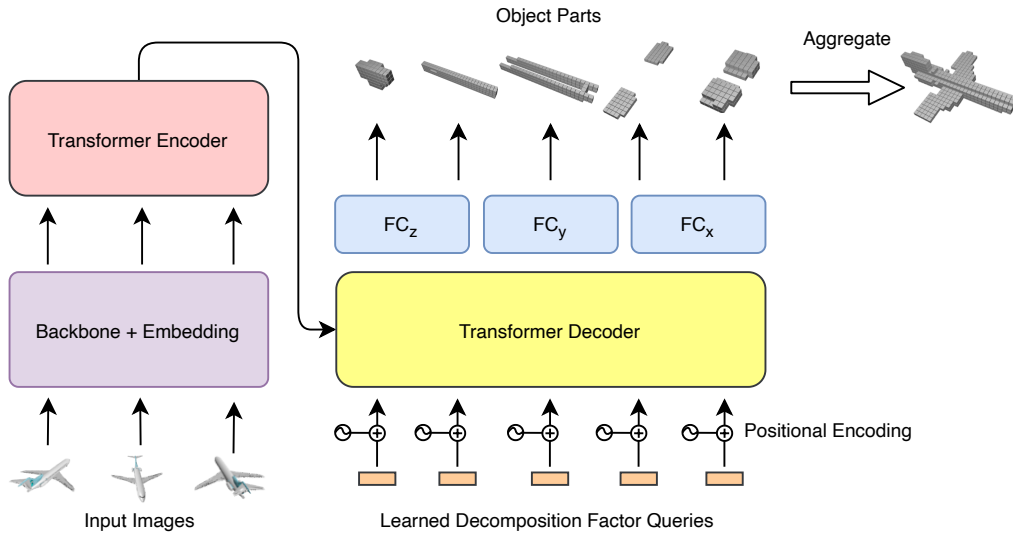


Figure 1: Overview of the LegoFormer architecture

has extended ViT with a spatiotemporal attention mechanism and achieves higher performance with less training time in video understanding tasks. More recently, hybrid approaches like LeViT [11] emerged where the convolutional blocks are integrated into the transformer model. Concurrently to our work [28] explored the use of a transformer-based model for 3D object reconstruction. Although there are similarities between the two works, our decoding scheme is significantly different. To the best of our knowledge, together with [28] we are the first work to explore the use of transformer-based models for 3D shape reconstruction.

**Compressed Representation** An efficient representation is crucial when working with fine detailed 3D objects. Techniques like Distance Field Compression [12], Octree [32] and Voxel Hashing [19] exploit sparseness of the voxel volume and offer 5-10 times compression [3]. These methods use specialized data structures that often require complex mapping to the original 3D volume. On the other hand, TT-TSDF [3] uses Low-Rank Tensor Train decomposition to represent the 3D tensor with lower rank tensors and demonstrates its application on the TSDF volumes. PARAFAC and Tucker are alternative general purpose decomposition algorithms where the latter has higher stability [3]. Modified algorithms for boolean matrix decomposition were proposed by [22] and [27] by introducing constraints over the decomposition factors. Matrix factorization is also used widely in recommendation systems to understand relationships [15]. The LegoFormer output representation is similar to the one in PARAFAC with a modification that bounds the decomposition factors in the range  $[0, 1]$  to ensure binary decomposition. Negative numbers are not included in the prediction range to avoid "deletion" of the object parts during the aggregation phase.

### 3 Methodology

#### 3.1 LegoFormer

**Overview** Figure 1 provides an overview of the proposed architecture. LegoFormer uses a vanilla pre-norm encoder/decoder transformer model [18] to reconstruct a 3D occupancy grid of size  $32^3$  from a set of 2D views. Each view is first mapped to an input token by a CNN-backbone. On the encoder side, the inputs are jointly encoded using the self-attention mechanism. Then the encoded inputs are passed to a non-autoregressive decoder together with a set of learned input queries. The decoder processes each query into a  $32^3$  volume containing a "part" of the full object. Each "part" volume is parametrized by three vectors and calculated as the outer product between them. The final occupancy grid is the sum of the predicted parts. We do not supervise the subdivision of the objects into parts during training, which emerges naturally, instead, thanks to the architecture and the

training objective formulation. Considering a single-view reconstruction the attention mechanism on the encoder side will not do anything with the formulation described so far. For this reason, we also propose a variant of our method tailored for the single view case, where the input tokens are obtained from the patches of a single view instead of the full image. We will refer to the two variants of our method as LegoFormer-M and LegoFormer-S for the multi- and single-view cases to differentiate between the two scenarios, respectively.

**Backbone and Embedding** Due to the high spatial dimensionality of the input 2D images ( $224 \times 224 \times 3$ ), it is not feasible to feed them directly into the transformer, which typically has a much lower dimensionality. Therefore we use a VGG16 [23] model, pre-trained on ImageNet [6], followed by  $c$  additional units of convolutional layers to map images to a compact feature representation  $\psi$ , as in [4, 31]. Each convolutional unit is followed by batch normalization and a ReLU activation. The pre-trained model weights are frozen during the training while the convolutional units are trained.

*LegoFormer-M*: uses  $c = 3$  convolution blocks with a MaxPool after the second block with kernel size 2. The output features have size  $\psi = 8 \times 8 \times 64$  and are flattened and then projected using a single fully connected layer to obtain the input tokens for the transformer model.

*LegoFormer-S*: uses  $c = 1$  convolution block that results in an output size  $\psi = 28 \times 28 \times 48$ . The input sequence for LegoFormer-S is defined as a set of square patches of size  $p = 4$  extracted from  $\psi$  resulting in  $\frac{28}{4} \cdot \frac{28}{4} = 49$  input tokens. Each patch is projected using a single fully connected layer to obtain the input tokens for the transformer.

**Encoding** We use a vanilla transformer encoder with pre-norm residual connections [18] to encode the input tokens. Each input token is allowed to attend to any other input while being encoded, so no self-attention mask is used. The pre-norm residual connections are preferred over post-norm connections due to the increased training stability. We do not use any positional encoding in LegoFormer-M to achieve input permutation invariance. Nevertheless, in LegoFormer-S we add to the input tokens a 2D positional sine-cos encoding [21] to inject the spatial relation between patches.

**Decoding** The decoder also uses the vanilla pre-norm transformer [18] and a non-autoregressive formulation where the predictions are made in parallel. Following DETR [4] we use learned decoder inputs, denoted decomposition factor queries, as input at the first decoder layer. The queries of the same size as the transformer dimensionality are initialized from a normal distribution with  $\mu = 0$  and  $\sigma = 1$ . In contrast to the encoder, an attention mask is applied to prevent queries from attending to themselves. We experimentally found that such masking leads to a slight increase in performance compared to no masking. A 1D positional sine-cos encoding [21] is added to each learned query before passing it to the decoder. This addition is necessary to help distinguish between queries and avoid the collapse of all outputs to the same value during training.

**Output** The raw decoder outputs  $Y_i$  are linearly projected using three fully connected layers  $FC_{\{z,y,x\}}$  into three vectors of size  $\mathbb{R}^{32}$  corresponding to the decomposition factor components. After applying a sigmoid activation  $\sigma$ , we use a cross-product between the vectors to obtain a rank-1 estimation of the entire voxel grid. Each query is decoded into a rank-1 estimation, and all of them are combined by sum-aggregation to obtain the final reconstruction  $P$ . Formally, this is defined as

$$\mathbf{z}_i, \mathbf{y}_i, \mathbf{x}_i = FC_3(Y_i) \tag{1}$$

$$\mathbf{z}_i, \mathbf{y}_i, \mathbf{x}_i = \sigma(\mathbf{z}_i), \sigma(\mathbf{y}_i), \sigma(\mathbf{x}_i) \tag{2}$$

$$P = \min(1, \sum_i \mathbf{z}_i \otimes \mathbf{y}_i \otimes \mathbf{x}_i) \tag{3}$$

As the target values are in the range  $[0, 1]$  the sigmoid is a suitable activation function. To prevent voxels with values larger than 1 after the sum-aggregation, we clip the aggregated volume. The clipping also replicates the rules of boolean algebra where  $1 + 1 = 1$  [16]

**Loss function** We use Mean-Squared-Error as the loss function to train the network. It is calculated between the predicted reconstruction and the ground-truth volume  $G$  as follows:

$$\mathcal{L}_{mse}(P, G) = \frac{1}{N^3} \sum_{i=0}^N \sum_{j=0}^N \sum_{k=0}^N (P_{i,j,k} - G_{i,j,k})^2 \quad (4)$$

### 3.2 Alternative Schemes

During the development of this work we explored several alternatives to the tensor decomposition-based schema for the decoder part of our network. The alternative approaches subdivide the output volume into fixed patches and predict each patch/voxel explicitly. Three such schemes are described below. Note that they are not related to LegoFormer and are only used for comparison in Sec. 4.5.

**Naive:** A simple approach for the output sequence subdivides the output volume into an ordered list of 3D patches of size  $4^3$  and predicts them sequentially using a transformer decoder in an auto-regressive fashion. A causal mask [26] for the decoder-side attention is used during the training to prevent the decoder inputs from attending to future elements of the sequence. Formally,

$$Y_i = \mathcal{D}(\mathcal{E}, P_{0\dots i-1}) \quad (5)$$

$$P_i = \sigma(FC(Y_i)) \quad (6)$$

$$P = \text{reshape}(P_0, P_1, \dots, P_n) \quad (7)$$

Where  $\mathcal{D}$  and  $\mathcal{E}$  are the transformer decoder and the encoded views, respectively. Afterward, the predicted 3D patches are stitched together to obtain the total volume.

**Naive-nAR:** The above approach will result in low throughput performance during the inference due to the patches being predicted one by one. An alternative way, denoted "Naive-nAR", is predicting all patches simultaneously using a non-autoregressive decoder, which will significantly decrease the inference time. Formally,

$$P_i = \sigma(FC(\mathcal{D}(\mathcal{E}, \mathbf{l}_i))) \quad (8)$$

$$P = \text{reshape}(P_0, P_1, \dots, P_n) \quad (9)$$

where  $\mathbf{l}_i$  is a learned query as in the LegoFormer and DETR [4].

**Naive-Full:** Predicting the output volume in patches is computationally expensive and not scalable. Given a grid of side 32 and a patch of side 4, it will take  $8^3 = 512$  predictions to cover the whole volume. Although transformers can efficiently attend to long sequences, the memory requirement grows quadratically [1] with the output sequence length. In order to reduce the number of predictions required, the whole volume can be predicted at once using a single learned query. However, this sacrifices the use of attention on the decoder. The scheme can be defined as,

$$P = \sigma(FC(\mathcal{D}(\mathcal{E}, \mathbf{l}))) \quad (10)$$

## 4 Experiments

### 4.1 Evaluation protocol and implementation details

**Dataset** Following [5, 30, 31] we use rendered images from ShapeNet [29] to evaluate the proposed method. To have comparable results, we follow the settings of [5] and use a subset of ShapeNet, which includes 43783 models from 13 categories. Each model is rendered from 24 different poses. The original images of size  $137 \times 137$  are resized to  $224 \times 224$  and a uniform background color is applied before passing them to the network. The ground truth targets are 3D occupancy grids with size  $32^3$  and target volumes aligned to a canonical reference frame.

**Metrics** 3D Intersection over Union (IoU) and F-score are used to measure the reconstruction performance. Given predicted  $\mathcal{R}$  and ground-truth  $\mathcal{G}$  occupancy volumes, the former measures the ratio of intersecting voxels from both volumes to their union. The ratio ensures that the calculation is object size independent. The latter metric, proposed by [14], focuses on the quality of the surface reconstruction and measures the percentage of points from the object surfaces that are closer than a predefined threshold. We follow the setup of [31] to convert the predicted volumes to point clouds and use the implementation provided by [25] for calculating the F-score. For both metrics, a higher value means better reconstruction.

Table 1: Comparison of multi-view reconstruction between models on ShapeNet at  $32^3$  resolution. Mean IoU and F-Score@1% reported for all categories.

Model	Number of Views								
	1	2	3	4	5	8	12	16	20
<b>Metric: IoU</b>									
3D-R2N2	0.560	0.603	0.617	0.625	0.634	0.635	0.636	0.636	0.636
AttSets	0.642	0.662	0.67	0.675	0.677	0.685	0.688	0.692	0.693
Pix2Vox/F	0.634	0.660	0.668	0.673	0.676	0.680	0.682	0.684	0.684
Pix2Vox/A	0.661	0.686	0.693	0.697	0.699	0.702	0.704	0.705	0.706
Pix2Vox++/F	0.645	0.669	0.678	0.682	0.685	0.690	0.692	0.693	0.694
Pix2Vox++/A	<b>0.670</b>	<b>0.695</b>	<b>0.704</b>	<b>0.708</b>	<b>0.711</b>	<b>0.715</b>	<b>0.717</b>	0.718	0.719
LegoFormer-M	0.519	0.644	0.679	0.694	0.703	0.713	<b>0.717</b>	<b>0.719</b>	<b>0.721</b>
LegoFormer-S	0.655	-	-	-	-	-	-	-	-
<b>Metric: F-score @ 1%</b>									
3D-R2N2	0.351	0.368	0.372	0.378	0.382	0.383	0.382	0.382	0.383
AttSets	0.395	0.418	0.426	0.430	0.432	0.444	0.445	0.447	0.448
Pix2Vox/F	0.364	0.393	0.404	0.409	0.412	0.417	0.420	0.423	0.423
Pix2Vox/A	0.405	0.435	0.448	0.449	0.452	0.456	0.458	0.459	0.460
Pix2Vox++/F	0.394	0.422	0.432	0.437	0.440	0.446	0.449	0.450	0.451
Pix2Vox++/A	<b>0.436</b>	<b>0.452</b>	<b>0.455</b>	<b>0.457</b>	<b>0.458</b>	0.459	0.460	0.461	0.462
LegoFormer-M	0.282	0.392	0.428	0.444	0.453	<b>0.464</b>	<b>0.470</b>	<b>0.472</b>	<b>0.473</b>
LegoFormer-S	0.404	-	-	-	-	-	-	-	-

**Implementation Details** Both LegoFormer-M and LegoFormer-S are trained with batch size 128 using  $224 \times 224$  RGB images as input and  $32^3$  voxelized reconstructions as output. The models are implemented using PyTorch-Lightning [9] and trained on Nvidia A100 and T4 GPUs on Google Cloud Platform (GCP) using Adagrad optimizer [8]. The learning rate is set to 0.01 with 10K warmup steps. For multi-view models, the number of input views is fixed to 8 during the training as we experimentally found that fixing the view count helps to achieve higher performance than updating it between steps (section 7.2). The views are randomly sampled out of 24 views at each iteration. The number of layers for both encoder and decoder is set to 8. The transformer dimensionality is set to 768 and 4096 for input token and feed-forward layer, respectively. After running ablation studies with different number of decoder queries in the section 7.1, the decoder input count is fixed to 12, meaning that the reconstructed volume is formed from 12 rank-1 estimations. At inference time after the sum-aggregation and clipping, we use a threshold  $\tau = 0.3$  to obtain the occupancy grid. LegoFormer-M is trained for 80K steps, while LegoFormer-S is trained for 160K steps. No learning rate decay was used. Obtaining the reconstructed volumes from the decomposition factors is implemented using Einstein Summation for efficient use of the memory. We use data and implementations along with pre-trained models provided by authors under the MIT License for comparison to other works. Our code is available at <https://github.com/faridyagubbayli/LegoFormer>.

## 4.2 Multi-view Reconstruction

We evaluate the multi-view reconstruction performance of LegoFormer-M against 3D-R2N2, AttSets, Pix2Vox, and Pix2Vox++. As shown in Table 1 the proposed method slightly outperforms other techniques when more than 12 views are given. The difference in F-score is higher than the difference

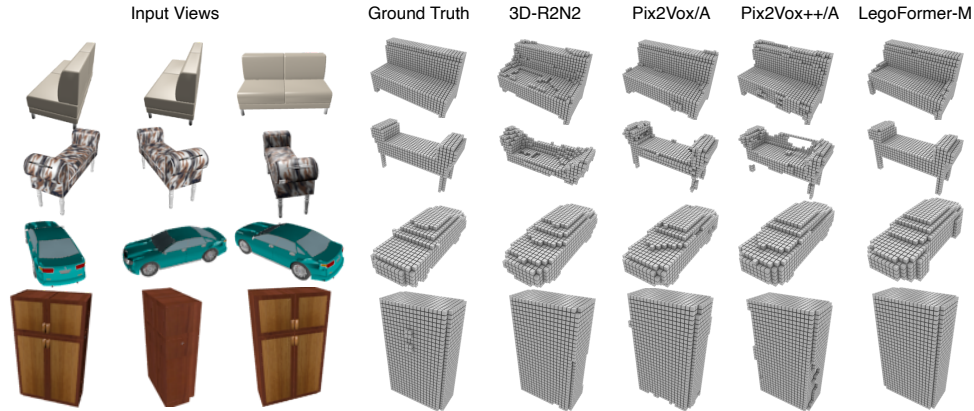


Figure 2: Multi-view object reconstructions for 4 input views (only 3 are shown) on ShapeNet with  $32^3$  resolution.

in IoU, meaning that LegoFormer reconstructs object surfaces better. The performance for the lower number of views is comparable to the state-of-the-art method Pix2Vox++ and the method outperforms 3D-R2N and AttSets when two or more views are given. Increasing the number of input views increases the performance of all methods, however for our method the gain is higher thanks to the use of the attention mechanism during the view encoding. For example, we get a +12.5 mIoU between not using encoder side attention (1 view) and using it (2 views), showing the impact of this component.

Fig. 2 displays example reconstructions obtained from 4 input views (only 3 are shown). In general, the reconstructions by LegoFormer tend to have less noise and smoother surfaces. This property can be attributed to the reconstruction via the tensor decomposition, where the output is an aggregation of rank-1 tensors defined by three vectors. The cross-product between three vectors makes it harder for the network to predict random spike-like voxels and acts as a regularizer that forces to reconstruct the object from well-connected chunks. A qualitative example of this can be the sitting and the backrest areas of the bench and sofa reconstructions.

### 4.3 Single-view Reconstruction

The first column of Table 1 also compares LegoFormer-S and LegoFormer-M against state-of-the-art methods for the object reconstruction. As expected LegoFormer-S, which uses image patches as input tokens, outperforms LegoFormer-M, which uses full images as tokens, showing the advantage of using the attention mechanism on the encoder again. Compared to other methods, LegoFormer-S shows competitive performance. Some examples of single view reconstruction are shown in Figure 3, highlighting how the shape predicted by LegoFormer-S is much smoother and more regular than the one predicted by the competitors. A category-wise comparison to the other single-view reconstruction techniques is reported in the supplementary section 8.

### 4.4 Model Analysis

One advantage of using LegoFormer is the increased interpretability of the reconstruction process. Analyzing and visualizing the attention scores gives insight on the way predictions are made. There are 3 types of attention: encoder-to-encoder, decoder-to-encoder and decoder-to-decoder. In the proposed architecture, the second gives information on where the network "looks" when reconstructing specific parts. The decoder-to-decoder attention instead helps to know which parts are taken into account when predicting a specific part of the object.

Figure 4 visualizes the attention scores for two examples from a LegoFormer model trained with 6-factor queries. We use a reduced number of queries for this experiment to ease the visualization. First, the network pays more attention to the airplane body while reconstructing its tail, likely because the tail can be predicted by looking at the plane's body. Second, when reconstructing a specific part, the surrounding parts get more attention. This can be observed in the last three columns for

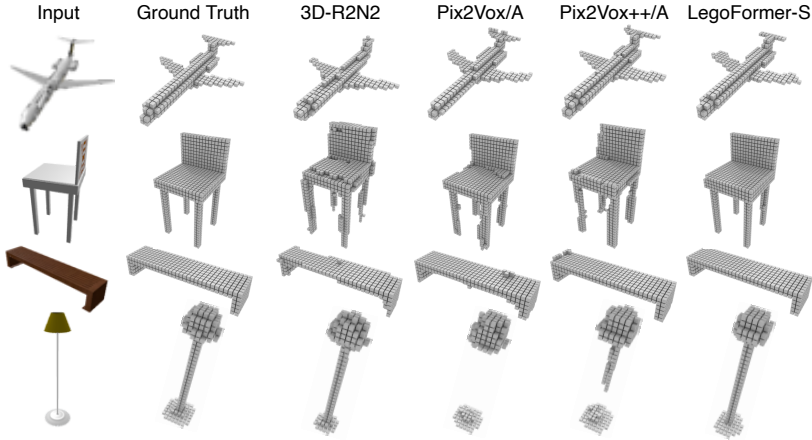


Figure 3: Single-view object reconstructions on ShapeNet with  $32^3$  resolution.

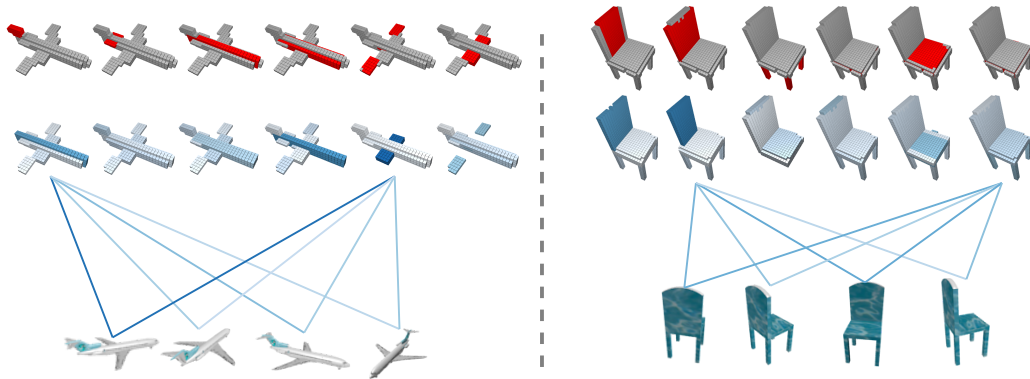


Figure 4: Decoder-to-encoder and decoder-to-decoder attention visualization for multi-view reconstruction using a LegoFormer-M model trained with 6 queries. Red color shows the part being reconstructed. Blue color denotes the attention score with darker meaning higher attention. The decoder attentions are given in range  $[0, 1]$  while decoder-to-encoder attentions in range  $[0, 0.60]$ . The latter is visualized for two queries for simplicity.

the airplane and the first two columns for the chair. Also, in case the part is divided into two or more pieces, like airplane wings and chair backrest from the examples, the other adjacent pieces get significantly higher attention. Consistency could be an explanation for these observations, i.e., the network tries to make sure that predicted parts fit together. Last but not least, one of the input views might get the majority of the attention from the decoder side. The multi-view performance metrics from the previous section justify this behavior since an object can be reconstructed from a single view with 0.61 IoU. Therefore a single view already contains most of the information used for the reconstruction, while additional views are mainly used for filling in the missing details.

Interestingly, we observed intra- and inter- category consistency in how the queries get decoded into object parts. Figure 5 displays reconstructions for 2 categories each with 2 examples. For the tables, the first queries predict the legs, while the last ones predict the top part in both examples. A similar pattern exists for chairs - the backrest gets predicted by the first queries followed by the legs and the seat. Furthermore, we observe some form of consistency between categories: the first queries tend to predict the legs and the sides of the object while the lasts predict the top plane and everything in the middle. These experimental observations suggest that during the training, the queries specialize on specific parts that are similar between objects from the same and different categories. This might indicate that the network has automatically learned to decompose the objects into parts with similar geometric or semantic structures.



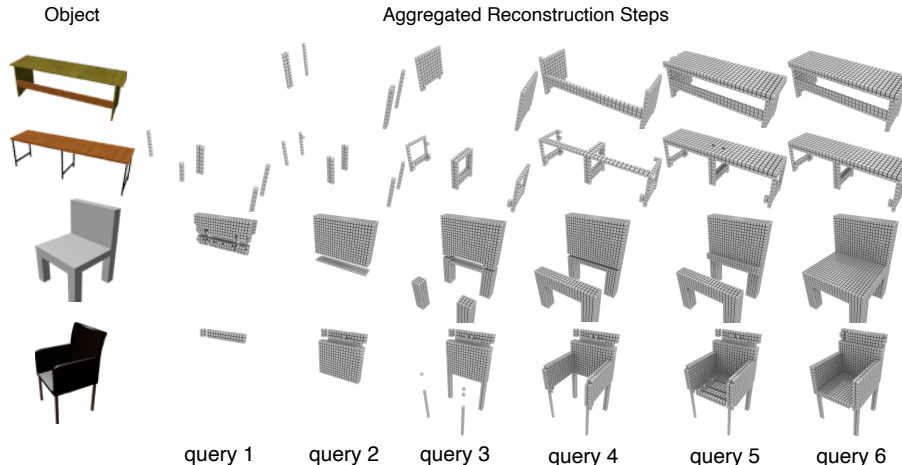


Figure 5: Aggregated reconstruction from a model trained with 6 queries on ShapeNet.

Table 2: Comparison of multi-view reconstruction performance of the decoding schemes on ShapeNet at  $32^3$  resolution. Mean IoU and F-Score@1% reported for all categories. All models are trained with 4 input views.

	IoU				F-Score@1%			
	Naive	Naive-nAR	Naive-Full	LegoFormer-M	Naive	Naive-nAR	Naive-Full	LegoFormer-M
1 view	0.500	0.557	0.558	<b>0.617</b>	0.290	0.333	0.337	<b>0.364</b>
2 views	0.552	0.640	0.643	<b>0.674</b>	0.339	<b>0.427</b>	0.426	0.422
3 views	0.567	0.663	0.659	<b>0.689</b>	0.353	<b>0.456</b>	0.447	0.438
4 views	0.573	0.670	0.668	<b>0.695</b>	0.359	<b>0.464</b>	0.458	0.445
5 views	0.577	0.676	0.672	<b>0.699</b>	0.363	<b>0.472</b>	0.463	0.449
8 views	0.582	0.681	0.675	<b>0.704</b>	0.367	<b>0.480</b>	0.467	0.455
12 views	0.583	0.685	0.680	<b>0.706</b>	0.369	<b>0.486</b>	0.474	0.457
16 views	0.584	0.686	0.681	<b>0.707</b>	0.371	<b>0.489</b>	0.477	0.459
20 views	0.585	0.687	0.681	<b>0.708</b>	0.372	<b>0.489</b>	0.476	0.459

#### 4.5 Comparison to other decoding schemes

We compare the LegoFormer with alternative decoding schemes in Table 2. The comparison is done among models trained with 4 input views. The LegoFormer achieves the highest IoU in all view counts while both "Naive-nAR" and "Naive-Full" have higher F-score performance suggesting that the former is better for objects with solid interior while the latter are good at reconstructing surfaces. The "Naive-nAR" decoding scheme constantly achieves the highest F-score except for a single view case where LegoFormer is better. Compared to LegoFormer, "Naive-nAR" solves an easier task where the subspace predicted by each query is predefined and doesn't change. However, the memory requirement is much higher, making it a less attractive solution when considering scaling the output to a higher resolution. Finally, "Naive-Full" is the most canonical architecture where the voxels predictions are direct outputs of the network decoder. This solution is still competitive but will suffer from the same scalability problem of "Naive-nAR" when increasing the output resolution. The "Naive" model has the worst performance, which can be attributed to accumulated error. As the predictions are made in sequence while conditioning on previous steps, a slight mistake at some early steps will result in wrong predictions later on. We observed a huge gap between train and test accuracy for this model, which leads us to conclude that autoregressive decoding schemes are not good candidates for 3D voxel grid reconstruction. An additional qualitative comparison of the decoding schemes is provided in the supplementary section 9.

## 5 Conclusion & Discussion

We presented a framework named LegoFormer that uses a transformer model to reconstruct an object from multiple views via its decomposition factors. The proposed method combines view encoding and volume prediction under the same tightly integrated network. In contrast to previous works where knowledge from all views is only available at the end of the encoding, in LegoFormer it is available at every step thanks to the attention mechanism. Moreover, we presented extensive insights on transformer-based decoding schemes for 3D reconstruction and shown the advantages of the reconstruction via attention-based tensor decomposition. Using this approach, a network can learn to predict independent object parts in an unsupervised manner. The proposed output scheme achieves competitive results on ShapeNet without requiring a refinement network as in the Pix2Vox and R2N2. Moreover, the analysis of the attention mechanism gives insights into the predictions.

Finally, several limitations of this work should be considered in the future. The output scheme has been explored only for the occupancy grids. While in theory, it can be extended to signed distance fields with minimal changes. Furthermore, the performance was measured regarding the output resolution  $32^3$ . The method can be adapted to higher resolutions by only changing the output dimensionality. However, a considerably larger dataset might be needed to train the model properly.

## 6 Acknowledgements

We thank Diego Martin Arroyo and Janis Postels for the discussions. We are also grateful to Google University Relationship GCP Credit Program for the support of this work by providing computational resources.

## References

- [1] Joshua Ainslie, Santiago Ontanón, Chris Alberti, Vaclav Cvicek, Zachary Fisher, Philip Pham, Anirudh Ravula, Sumit Sanghai, Qifan Wang, and Li Yang. “ETC: Encoding Long and Structured Inputs in Transformers”. In: *arXiv preprint arXiv:2004.08483* (2020).
- [2] Gedas Bertasius, Heng Wang, and Lorenzo Torresani. “Is Space-Time Attention All You Need for Video Understanding?” In: *arXiv preprint arXiv:2102.05095* (2021).
- [3] Alexey I Boyko, Mikhail P Matrosov, Ivan V Oseledets, Dzmitry Tsetserukou, and Gonzalo Ferrer. “TT-TSDF: Memory-Efficient TSDF with Low-Rank Tensor Train Decomposition”. In: ().
- [4] Nicolas Carion, Francisco Massa, Gabriel Synnaeve, Nicolas Usunier, Alexander Kirillov, and Sergey Zagoruyko. “End-to-end object detection with transformers”. In: *European Conference on Computer Vision*. Springer, 2020, pp. 213–229.
- [5] Christopher B Choy, Danfei Xu, JunYoung Gwak, Kevin Chen, and Silvio Savarese. “3d-r2n2: A unified approach for single and multi-view 3d object reconstruction”. In: *European conference on computer vision*. Springer, 2016, pp. 628–644.
- [6] Jia Deng, Wei Dong, Richard Socher, Li-Jia Li, Kai Li, and Li Fei-Fei. “Imagenet: A large-scale hierarchical image database”. In: *2009 IEEE conference on computer vision and pattern recognition*. Ieee, 2009, pp. 248–255.
- [7] Alexey Dosovitskiy, Lucas Beyer, Alexander Kolesnikov, Dirk Weissenborn, Xiaohua Zhai, Thomas Unterthiner, Mostafa Dehghani, Matthias Minderer, Georg Heigold, Sylvain Gelly, et al. “An image is worth 16x16 words: Transformers for image recognition at scale”. In: *arXiv preprint arXiv:2010.11929* (2020).
- [8] John Duchi, Elad Hazan, and Yoram Singer. “Adaptive subgradient methods for online learning and stochastic optimization.” In: *Journal of machine learning research* 12.7 (2011).
- [9] et al. Falcon WA. “PyTorch Lightning”. In: *GitHub*. Note: <https://github.com/PyTorchLightning/pytorch-lightning> 3 (2019).
- [10] Jorge Fuentes-Pacheco, José Ruiz-Ascencio, and Juan Manuel Rendón-Mancha. “Visual simultaneous localization and mapping: a survey”. In: *Artificial intelligence review* 43.1 (2015), pp. 55–81.

- [11] Ben Graham, Alaaeldin El-Nouby, Hugo Touvron, Pierre Stock, Armand Joulin, Hervé Jégou, and Matthijs Douze. “LeViT: a Vision Transformer in ConvNet’s Clothing for Faster Inference”. In: *arXiv preprint arXiv:2104.01136* (2021).
- [12] Mark W Jones. “Distance field compression”. In: (2004).
- [13] Abhishek Kar, Christian Häne, and Jitendra Malik. “Learning a multi-view stereo machine”. In: *arXiv preprint arXiv:1708.05375* (2017).
- [14] Arno Knapitsch, Jaesik Park, Qian-Yi Zhou, and Vladlen Koltun. “Tanks and temples: Benchmarking large-scale scene reconstruction”. In: *ACM Transactions on Graphics (ToG)* 36.4 (2017), pp. 1–13.
- [15] Yehuda Koren, Robert Bell, and Chris Volinsky. “Matrix factorization techniques for recommender systems”. In: *Computer* 42.8 (2009), pp. 30–37.
- [16] Pauli Miettinen and Stefan Neumann. “Recent developments in boolean matrix factorization”. In: *arXiv preprint arXiv:2012.03127* (2020).
- [17] Ramakant Nevatia and Thomas O Binford. “Description and recognition of curved objects”. In: *Artificial intelligence* 8.1 (1977), pp. 77–98.
- [18] Toan Q Nguyen and Julian Salazar. “Transformers without tears: Improving the normalization of self-attention”. In: *arXiv preprint arXiv:1910.05895* (2019).
- [19] Matthias Nießner, Michael Zollhöfer, Shahram Izadi, and Marc Stamminger. “Real-time 3D reconstruction at scale using voxel hashing”. In: *ACM Transactions on Graphics (ToG)* 32.6 (2013), pp. 1–11.
- [20] Onur Ozyesil, Vladislav Voroninski, Ronen Basri, and Amit Singer. “A survey of structure from motion”. In: *arXiv preprint arXiv:1701.08493* (2017).
- [21] Niki Parmar, Ashish Vaswani, Jakob Uszkoreit, Lukasz Kaiser, Noam Shazeer, Alexander Ku, and Dustin Tran. “Image transformer”. In: *International Conference on Machine Learning*. PMLR, 2018, pp. 4055–4064.
- [22] Tammo Rukat, Chris C Holmes, and Christopher Yau. “Tensormachine: probabilistic Boolean tensor decomposition”. In: *arXiv preprint arXiv:1805.04582* (2018).
- [23] Karen Simonyan and Andrew Zisserman. “Very deep convolutional networks for large-scale image recognition”. In: *arXiv preprint arXiv:1409.1556* (2014).
- [24] Riccardo Spezialetti, David Joseph Tan, Alessio Tonioni, Keisuke Tateno, and Federico Tombari. “A Divide et Impera Approach for 3D Shape Reconstruction from Multiple Views”. In: *arXiv preprint arXiv:2011.08534* (2020).
- [25] Maxim Tatarchenko, Stephan R Richter, René Ranftl, Zhuwen Li, Vladlen Koltun, and Thomas Brox. “What do single-view 3d reconstruction networks learn?” In: *Proceedings of the IEEE/CVF Conference on Computer Vision and Pattern Recognition*. 2019, pp. 3405–3414.
- [26] Ashish Vaswani, Noam Shazeer, Niki Parmar, Jakob Uszkoreit, Llion Jones, Aidan N Gomez, Lukasz Kaiser, and Illia Polosukhin. “Attention is all you need”. In: *arXiv preprint arXiv:1706.03762* (2017).
- [27] Changlin Wan, Wennan Chang, Tong Zhao, Sha Cao, and Chi Zhang. “Geometric All-Way Boolean Tensor Decomposition”. In: *arXiv preprint arXiv:2007.15821* (2020).
- [28] Dan Wang, Xinrui Cui, Xun Chen, Zhengxia Zou, Tianyang Shi, Septimiu Salcudean, Z Jane Wang, and Rabab Ward. “Multi-view 3D Reconstruction with Transformer”. In: *arXiv preprint arXiv:2103.12957* (2021).
- [29] Zhirong Wu, Shuran Song, Aditya Khosla, Fisher Yu, Linguang Zhang, Xiaoou Tang, and Jianxiong Xiao. “3d shapenets: A deep representation for volumetric shapes”. In: *Proceedings of the IEEE conference on computer vision and pattern recognition*. 2015, pp. 1912–1920.
- [30] Haozhe Xie, Hongxun Yao, Xiaoshuai Sun, Shangchen Zhou, and Shengping Zhang. “Pix2vox: Context-aware 3d reconstruction from single and multi-view images”. In: *Proceedings of the IEEE/CVF International Conference on Computer Vision*. 2019, pp. 2690–2698.
- [31] Haozhe Xie, Hongxun Yao, Shengping Zhang, Shangchen Zhou, and Wenxiu Sun. “Pix2Vox++: multi-scale context-aware 3D object reconstruction from single and multiple images”. In: *International Journal of Computer Vision* 128.12 (2020), pp. 2919–2935.
- [32] Ming Zeng, Fukai Zhao, Jiayang Zheng, and Xinguo Liu. “Octree-based fusion for realtime 3D reconstruction”. In: *Graphical Models* 75.3 (2013), pp. 126–136.

- [33] M Zeeshan Zia, M Stark, B Schiele, and K Schindler. “Detailed 3d representations for object modeling and recognition”. In: *IEEE Transactions on Pattern Analysis and Machine Intelligence* 35.11 (2013), pp. 2608–2623.

---

# Supplementary Material for LegoFormer: Transformers for Block-by-Block Multi-view 3D Reconstruction

---

**Farid Yagubbayli**<sup>1</sup>  
farid.yagubbayli@tum.de

**Alessio Tonioni**<sup>2</sup>  
alessiot@google.com

**Federico Tombari**<sup>1,2</sup>  
tombari@in.tum.de

<sup>1</sup>Technical University of Munich

<sup>2</sup>Google Inc.

## 7 Additional ablation tests

We report here additional ablation studies to highlight the effect of different hyperparameters on the performance of the proposed architectures.

### 7.1 Number of Decomposition Factors

In LegoFormer, the output volume is formed as a sum of  $n$  rank-1 approximations obtained by independently processing  $n$  learned queries. The number of approximations considered is related to the reconstruction performance achievable. Table 3 lists the performance of models trained with a different number of output queries against a different number of input views considered at test time. For each query count, the model was trained from scratch. As it can be easily observed, increasing the number of queries corresponds to an increase in performance—however, the increase stalls after 12 queries. Interestingly, with only 2 queries a good IoU and F1-score performance can be achieved, only around 5 points lower than the best configurations. This means that our architecture can approximate very complex object shapes using as few as two rank-1 approximations.

### 7.2 Training with different view counts

We also study the effect of the number of input views considered during training the LegoFormer-M model. We considered both using a fixed view count (2, 4 or 8) as well as random sampling the number of input views considered at every training iteration. Table 4 reports the results of these experiments. First of all, we can notice how, for the fixed number of inputs, there is a loose correlation between the number of training views and the performance at test time. Indeed, a model trained with few inputs performs better when running inference on few views and vice versa. This can be observed comparing the performance of the model trained with 4 and 8 views, the former outperforms the latter for any inference views count lower than 4, but after this threshold, the latter model performs better. By training with a dynamic number of views, we tried to achieve higher performance regardless of view count during the evaluation. Unfortunately, we observed harder convergence with this setup resulting in lower performance. This could be linked to the instability problems of the transformer training [5].

### 7.3 Reducing model dimensionality

The parameter count of the transformer models can grow pretty quickly, resulting in higher memory requirements. A number of techniques were proposed to counteract the parameter growth of transformer architectures. One of the techniques is to share weights between transformer encoder and decoder layers, as proposed in ALBERT [4]. Using this technique, only a single transformer layer is

Table 3: Comparison of the reconstruction performance with respect to the number of queries used on the decoder side. For each number of queries a separate model was trained from scratch.

View count	Query count						
	2	3	4	6	8	12	16
<b>IoU</b>							
1 view	0.585	0.598	0.606	0.609	0.611	<b>0.617</b>	0.614
2 views	0.627	0.648	0.656	0.663	0.668	<b>0.674</b>	<b>0.674</b>
3 views	0.637	0.661	0.669	0.679	0.684	<b>0.689</b>	<b>0.689</b>
4 views	0.643	0.667	0.675	0.685	0.690	<b>0.695</b>	<b>0.695</b>
5 views	0.646	0.670	0.679	0.689	0.694	<b>0.699</b>	<b>0.699</b>
8 views	0.650	0.675	0.684	0.694	0.700	<b>0.704</b>	<b>0.704</b>
12 views	0.652	0.677	0.685	0.697	0.702	0.706	<b>0.707</b>
16 views	0.653	0.678	0.687	0.698	0.703	0.707	<b>0.708</b>
20 views	0.653	0.679	0.687	0.699	0.704	0.708	<b>0.709</b>
<b>F-Score @ 1%</b>							
1 view	0.323	0.336	0.345	0.355	0.358	<b>0.364</b>	0.362
2 views	0.362	0.383	0.392	0.407	0.413	<b>0.422</b>	0.421
3 views	0.373	0.397	0.407	0.424	0.429	<b>0.438</b>	<b>0.438</b>
4 views	0.379	0.402	0.413	0.430	0.436	<b>0.445</b>	0.444
5 views	0.382	0.406	0.417	0.434	0.441	<b>0.449</b>	<b>0.449</b>
8 views	0.386	0.411	0.422	0.440	0.447	<b>0.455</b>	<b>0.455</b>
12 views	0.389	0.414	0.424	0.443	0.451	0.457	<b>0.458</b>
16 views	0.389	0.415	0.425	0.445	0.452	<b>0.459</b>	<b>0.459</b>
20 views	0.390	0.415	0.426	0.445	0.453	0.459	<b>0.461</b>

Table 4: Effect of the number of input views used during training on the inference-time performance on the ShapeNet dataset at  $32^3$  resolution. In the setup of the column [1, 10) view count is changed at every iteration to a number between 1 and 9, inclusive. We also report the performance of the strongest competitor, Pix2Vox++/A [12] as a reference.

Training view count	Evaluation view count								
	1	2	3	4	5	8	12	16	20
<b>Metric: IoU</b>									
2	0.635	0.668	0.677	0.681	0.684	0.688	0.690	0.691	0.691
4	0.617	0.674	0.689	0.695	0.699	0.704	0.706	0.707	0.708
8	0.519	0.644	0.679	0.694	0.703	0.713	<b>0.717</b>	<b>0.719</b>	<b>0.721</b>
[1, 10)	0.601	0.638	0.652	0.659	0.663	0.669	0.672	0.673	0.674
Pix2Vox++/A [12]	<b>0.670</b>	<b>0.695</b>	<b>0.704</b>	<b>0.708</b>	<b>0.711</b>	<b>0.715</b>	<b>0.717</b>	0.718	0.719
<b>F-score @ 1%</b>									
2	0.377	0.412	0.421	0.426	0.428	0.433	0.435	0.436	0.437
4	0.364	0.422	0.438	0.445	0.449	0.455	0.457	0.459	0.459
8	0.282	0.392	0.428	0.444	0.453	<b>0.464</b>	<b>0.470</b>	<b>0.472</b>	<b>0.473</b>
[1, 10)	0.349	0.384	0.398	0.404	0.409	0.415	0.418	0.419	0.420
Pix2Vox++/A [12]	<b>0.436</b>	<b>0.452</b>	<b>0.455</b>	<b>0.457</b>	<b>0.458</b>	0.459	0.460	0.461	0.462

defined for the encoder and decoder, and the layer is repeatedly applied to the input. Weight sharing between layers significantly reduces the model size by 5.5 times, from 168M to 30.6M parameters, while experiencing minor performance drop as reported in Table 5. Based on this experiment, we show that there exist a nice trade-off between memory requirement and performance for LegoFormer architectures, and the former can be decreased significantly without affecting the latter much.

Table 5: Comparison between a vanilla LegoFormer and a parameter sharing LegoFormer on the ShapeNet dataset. In the latter case, all layers of the encoder and decoder use the same parameters, meaning that a single layer is repeatedly applied for each side resulting in using  $5.5x$  less parameters.

Setup		IoU			F-Score@1%		
		Vanilla	Parameter Sharing	Difference	Vanilla	Parameter Sharing	Difference
View	Count						
	1 view	<b>0.617</b>	0.596	-0.021	<b>0.364</b>	0.345	-0.019
	2 views	<b>0.674</b>	0.661	-0.013	<b>0.422</b>	0.406	-0.016
	3 views	<b>0.689</b>	0.678	-0.011	<b>0.438</b>	0.424	-0.014
	4 views	<b>0.695</b>	0.685	-0.010	<b>0.445</b>	0.432	-0.013
	5 views	<b>0.699</b>	0.691	-0.008	<b>0.449</b>	0.438	-0.011
	8 views	<b>0.704</b>	0.697	-0.007	<b>0.455</b>	0.444	-0.011
	12 views	<b>0.706</b>	0.700	-0.006	<b>0.457</b>	0.448	-0.009
	16 views	<b>0.707</b>	0.701	-0.006	<b>0.459</b>	0.449	-0.010
	20 views	<b>0.708</b>	0.702	-0.006	<b>0.459</b>	0.450	-0.009

## 8 Single view performance per category

Table 6 compares the single-view reconstruction performance of LegoFormer against 10 recent state-of-the-art methods that predict voxel grids [11, 12, 2, 8, 7], triangle meshes [3, 10] or implicit representations [6, 1]. We report both category-wise performance and "overall", i.e., the average over the available classes for each method. In almost every category, LegoFormer-S shows competitive performance against the other methods. Also, LegoFormer-S performs significantly better than LegoFormer-M in all categories, showing the importance of using attention-based encoding. Overall, the proposed method is competitive with recent proposals in the literature, outperforming several of them.

## 9 Comparison to other decoding schemes - Qualitative Results

In Figure 6 we show some qualitative examples of reconstructions using the different decoding schemes discussed in Section 3.2 of the main paper. In contrast to the naive approaches where the voxels are independently predicted, LegoFormer outputs are more structured and do not contain spike-like spurious full voxels (e.g., the small artifacts on the bottom right corner of the lamp reconstructed by Naive-Full). This observation supports our claim that using a tensor decomposition-based parametrization acts like a regularization and constrains the output space. The second row in the figure, is a relatively hard case for all approaches due to the unusual positioning of the armrests on the bench. While no model correctly reconstructs the 3D shape, all predictions are significantly noisier than the one obtained by LegoFormer-M. The same can be said of the reconstructed sofa in the first row, where all alternatives struggle to generate nice flat surfaces except for LegoFormer-M.

Table 6: Comparison of single-view reconstruction between models on ShapeNet at 32<sup>3</sup> resolution. Mean IoU and F-Score@1% reported for all categories.

Category	Method		3D-R2N2 [2]	OGN [8]	Matyoshka [7]	AtlasNet [3]	Pixel2Mesh [10]	OccNet [6]	IM-Net [1]	AttSets [13]	Pix2Vox/F [11]	Pix2Vox/A [11]	Pix2Vox++/F [12]	Pix2Vox++/A [12]	LegoFormer-M	LegoFormer-S
	IoU	F-Score@1%														
airplane	0.513	0.587	0.647	0.493	0.508	0.532	<b>0.702</b>	0.594	0.600	0.684	0.607	0.674	0.480	0.641		
bench	0.421	0.481	0.577	0.431	0.379	0.597	0.564	0.552	0.538	<b>0.616</b>	0.544	0.608	0.326	0.612		
cabinet	0.716	0.729	0.776	0.257	0.732	0.674	0.680	0.783	0.765	0.792	0.782	<b>0.799</b>	0.640	0.780		
car	0.798	0.828	0.850	0.282	0.670	0.671	0.756	0.844	0.837	0.854	0.841	<b>0.858</b>	0.724	0.852		
chair	0.466	0.483	0.547	0.328	0.484	0.583	<b>0.644</b>	0.559	0.535	0.567	0.548	0.581	0.442	0.557		
display	0.468	0.502	0.532	0.457	0.582	<b>0.651</b>	0.585	0.565	0.511	0.537	0.529	0.548	0.391	0.524		
lamp	0.381	0.398	0.408	0.261	0.399	<b>0.474</b>	0.433	0.445	0.435	0.443	0.448	0.457	0.428	0.453		
speaker	0.662	0.637	0.701	0.296	0.672	0.655	0.683	0.721	0.707	0.714	0.721	<b>0.721</b>	0.645	0.712		
rifle	0.544	0.593	0.616	0.573	0.468	0.656	<b>0.723</b>	0.601	0.598	0.615	0.594	0.617	0.465	0.632		
sofa	0.628	0.646	0.681	0.354	0.622	0.669	0.694	0.703	0.687	0.709	0.696	<b>0.725</b>	0.483	0.707		
table	0.513	0.536	0.573	0.301	0.536	<b>0.659</b>	0.621	0.590	0.587	0.601	0.609	0.620	0.489	0.596		
telephone	0.661	0.702	0.756	0.543	0.762	0.794	0.762	0.743	0.77	0.776	0.782	<b>0.809</b>	0.569	0.787		
watercraft	0.513	0.632	0.591	0.355	0.471	0.579	0.607	0.601	0.582	0.594	0.583	0.603	0.467	<b>0.608</b>		
overall	0.560	0.596	0.635	0.352	0.552	0.626	0.659	0.642	0.634	0.661	0.645	<b>0.670</b>	0.519	0.655		
<b>F-Score@1%</b>																
airplane	0.412	0.487	0.446	0.415	0.376	0.494	<b>0.598</b>	0.489	-	-	0.493	0.583	0.349	0.501		
bench	0.345	0.364	0.424	0.439	0.313	0.318	0.361	0.406	-	-	0.399	<b>0.478</b>	0.229	0.459		
cabinet	0.327	0.316	0.381	0.350	<b>0.450</b>	0.449	0.345	0.367	-	-	0.363	0.408	0.254	0.391		
car	0.481	0.514	0.481	0.319	0.486	0.315	0.304	0.497	-	-	0.523	<b>0.564</b>	0.364	0.525		
chair	0.238	0.226	0.302	0.406	0.386	0.365	<b>0.442</b>	0.334	-	-	0.262	0.309	0.193	0.269		
display	0.227	0.215	0.400	0.451	0.319	<b>0.468</b>	0.466	0.310	-	-	0.253	0.296	0.187	0.274		
lamp	0.267	0.249	0.276	0.217	0.219	0.361	<b>0.371</b>	0.315	-	-	0.287	0.315	0.289	0.307		
speaker	0.231	0.225	<b>0.279</b>	0.199	0.190	0.249	0.200	0.211	-	-	0.256	0.152	0.218	0.278		
rifle	0.521	0.541	0.514	0.405	0.340	0.219	0.407	0.524	-	-	0.553	<b>0.574</b>	0.417	0.563		
sofa	0.274	0.290	0.326	0.337	0.343	0.324	0.354	0.334	-	-	0.320	<b>0.377</b>	0.192	0.367		
table	0.340	0.352	0.374	0.373	0.502	<b>0.549</b>	0.461	0.419	-	-	0.385	0.406	0.276	0.369		
telephone	0.504	0.528	0.598	0.545	0.485	0.273	0.423	0.469	-	-	0.588	<b>0.633</b>	0.355	0.572		
watercraft	0.305	0.328	0.360	0.296	0.266	0.347	0.369	0.315	-	-	0.346	<b>0.390</b>	0.274	0.386		
overall	0.351	0.368	0.391	0.362	0.398	0.393	0.405	0.395	-	-	0.394	<b>0.436</b>	0.282	0.404		



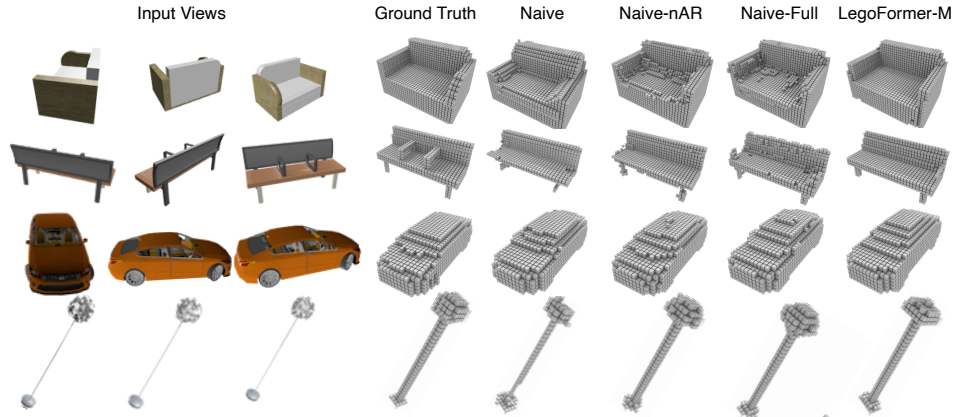


Figure 6: Multi-view object reconstructions of the four decoding schemes for 3 input views on ShapeNet with  $32^3$  resolution. The second row shows an example of a challenging case for all decoding schemes.

## 10 Comparison to Multi-view 3D Reconstruction with Transformer [9]

Wang et al. [9] is a work concurrent to ours that appeared on arXiv at the end of March 2021 and, to the best of our knowledge, is still unpublished. Since both [9] and our work share the idea of using transformers for 3D multi-view reconstructions we propose here a preliminary comparison, with the caveat of being based on a pre-print version of [9] with no code available. In [9], the encoder side of the transformer takes full views as input, as we do, but uses a different attention mechanism to foster different representations for each view. On the decoder side, instead, they stick to a more vanilla transformer formulation and use a decoding schema similar to our Naive-nAR as described in Section 3.2 on the main paper.

In Table 7 we report the performance of three variants of the method proposed in [9] (rows 1,2,3) and two variants of our model trained with a different number of input views. We can see how our formulation is competitive or outperforming [9] for a low view count, while for an high view count we perform slightly worse than EVoIT but better than the other variants. Among the three variants of [9] EVoIT is the only one using an enhanced attention schema. We believe that these experimental results show how our decoding schema is more effective than the one used in [9] while their enhanced attention helps in the case of many views provided as input. These insights pave the way to future developments where we will try to combine the two improvements.

Finally, while [9] proposes only models tailored for inference on many input views, we preferred to focus on the more challenging settings using few input views, up to the extreme of LegoFormer-S where just a single view is needed.

## 11 Visualizing Single-view Attention

The main paper shows the decoder-to-encoder attention maps between reconstructed blocks and input views for the multi-view setting (LegoFormer-M). Figure 7 reports the same for a single view input using the LegoFormer-S model. We use a special version of LegoFormer-S trained using input patches of size  $1^2$  instead of  $4^2$  as in the main paper for this test. The attention maps give insights into where the network "looks" when predicting a particular block. First, as expected, the attention is always higher on the object and surrounding parts. Attending to the surrounding parts could be helpful for the network to understand the boundary of the object. Second, the attention can be focused on a particular place or distributed over a larger area. For example, while predicting the tail of the plane (first and second row), the attention is spread all over the plane's body. In contrast, while reconstructing the chair legs (third row), the network attends only to relevant pixels and does not consider the chair's body. The reason behind this variation could be that the shape of the plane tails have higher variance, and "looking" to other parts is helpful, while the chair legs are more or

Table 7: Comparison to the concurrent work by Wang et al. [9] including three variations of their proposed architecture.

Model	Evaluation view count						
	4	6	8	12	16	20	24
<b>IoU</b>							
VolT [9]	0.605	0.662	0.681	0.699	0.706	0.711	0.714
VolT+ [9]	0.695	0.704	0.707	0.711	0.714	0.715	0.716
EVolT [9]	0.609	0.675	0.698	<b>0.720</b>	<b>0.729</b>	<b>0.735</b>	<b>0.738</b>
LegoFormer-M	<b>0.694</b>	<b>0.709</b>	<b>0.713</b>	0.717	0.719	0.721	0.721
<b>F-Score@1%</b>							
VolT [9]	0.356	0.410	0.430	0.450	0.459	0.464	0.468
VolT+ [9]	<b>0.451</b>	<b>0.460</b>	<b>0.464</b>	0.469	0.472	0.474	0.475
EVolT [9]	0.358	0.423	0.448	<b>0.475</b>	<b>0.486</b>	<b>0.492</b>	<b>0.497</b>
LegoFormer-M	0.444	<b>0.460</b>	<b>0.464</b>	0.470	0.472	0.473	0.474

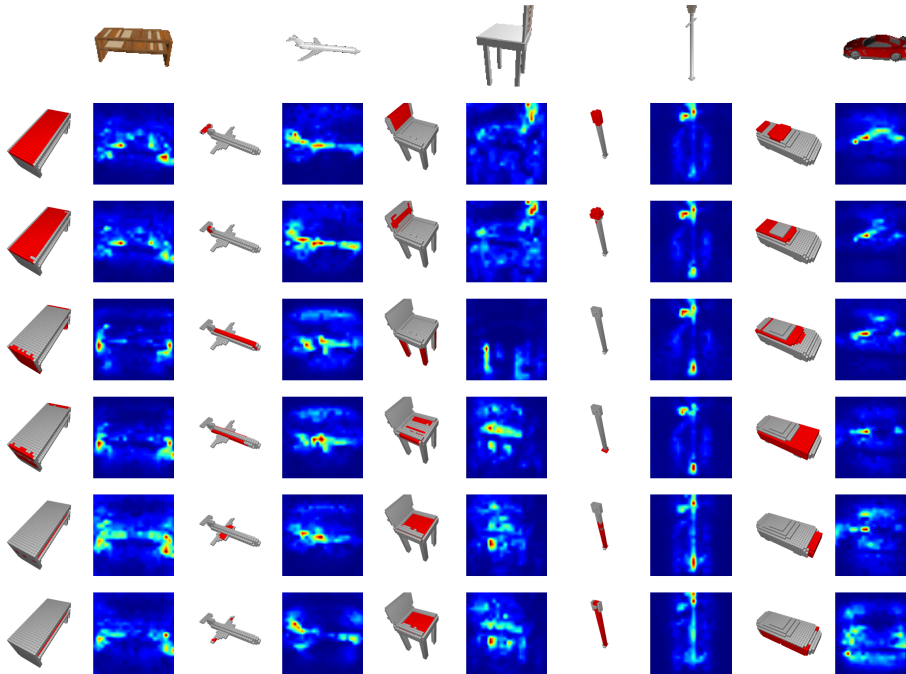


Figure 7: Visualization of the Decoder-to-Encoder attention for single view reconstruction obtained by a LegoFormer-S trained with input patch size  $1^2$ . The input image is shown in the top row. Odd columns show the part being reconstructed from a specific query (in red), while even columns plot the attention on the input image pixels. The attention maps are normalized into  $[0, 1]$  range and plotted using a jet colormap from red (high attention) to blue (low attention). No clipping is applied.

less similar to each other and self-sufficient for the reconstruction. Lastly, the decoder attends to similar parts of the images when reconstructing nearby blocks. For example, when reconstructing the central parts of the sitting of the chair (row 5 and 6) the attention maps generated look quite similar, indicating a strong relationship between the shape being generated and on which part of the input view the model decides to attend.

## References

- [1] Zhiqin Chen and Hao Zhang. “Learning implicit fields for generative shape modeling”. In: *Proceedings of the IEEE/CVF Conference on Computer Vision and Pattern Recognition*. 2019, pp. 5939–5948.
- [2] Christopher B Choy, Danfei Xu, JunYoung Gwak, Kevin Chen, and Silvio Savarese. “3d-r2n2: A unified approach for single and multi-view 3d object reconstruction”. In: *European conference on computer vision*. Springer. 2016, pp. 628–644.
- [3] Thibault Groueix, Matthew Fisher, Vladimir G Kim, Bryan C Russell, and Mathieu Aubry. “A papier-mâché approach to learning 3d surface generation”. In: *Proceedings of the IEEE conference on computer vision and pattern recognition*. 2018, pp. 216–224.
- [4] Zhenzhong Lan, Mingda Chen, Sebastian Goodman, Kevin Gimpel, Piyush Sharma, and Radu Soricut. “Albert: A lite bert for self-supervised learning of language representations”. In: *arXiv preprint arXiv:1909.11942* (2019).
- [5] Liyuan Liu, Xiaodong Liu, Jianfeng Gao, Weizhu Chen, and Jiawei Han. “Understanding the difficulty of training transformers”. In: *arXiv preprint arXiv:2004.08249* (2020).
- [6] Lars Mescheder, Michael Oechsle, Michael Niemeyer, Sebastian Nowozin, and Andreas Geiger. “Occupancy networks: Learning 3d reconstruction in function space”. In: *Proceedings of the IEEE/CVF Conference on Computer Vision and Pattern Recognition*. 2019, pp. 4460–4470.
- [7] Stephan R Richter and Stefan Roth. “Matryoshka networks: Predicting 3d geometry via nested shape layers”. In: *Proceedings of the IEEE conference on computer vision and pattern recognition*. 2018, pp. 1936–1944.
- [8] Maxim Tatarchenko, Alexey Dosovitskiy, and Thomas Brox. “Octree generating networks: Efficient convolutional architectures for high-resolution 3d outputs”. In: *Proceedings of the IEEE International Conference on Computer Vision*. 2017, pp. 2088–2096.
- [9] Dan Wang, Xinrui Cui, Xun Chen, Zhengxia Zou, Tianyang Shi, Septimiu Salcudean, Z Jane Wang, and Rabab Ward. “Multi-view 3D Reconstruction with Transformer”. In: *arXiv preprint arXiv:2103.12957* (2021).
- [10] Nanyang Wang, Yinda Zhang, Zhuwen Li, Yanwei Fu, Wei Liu, and Yu-Gang Jiang. “Pixel2mesh: Generating 3d mesh models from single rgb images”. In: *Proceedings of the European Conference on Computer Vision (ECCV)*. 2018, pp. 52–67.
- [11] Haozhe Xie, Hongxun Yao, Xiaoshuai Sun, Shangchen Zhou, and Shengping Zhang. “Pix2vox: Context-aware 3d reconstruction from single and multi-view images”. In: *Proceedings of the IEEE/CVF International Conference on Computer Vision*. 2019, pp. 2690–2698.
- [12] Haozhe Xie, Hongxun Yao, Shengping Zhang, Shangchen Zhou, and Wenxiu Sun. “Pix2Vox++: multi-scale context-aware 3D object reconstruction from single and multiple images”. In: *International Journal of Computer Vision* 128.12 (2020), pp. 2919–2935.
- [13] Bo Yang, Sen Wang, Andrew Markham, and Niki Trigoni. “Robust attentional aggregation of deep feature sets for multi-view 3D reconstruction”. In: *International Journal of Computer Vision* 128.1 (2020), pp. 53–73.